THE JOURNAL OF GENE MEDICINE
J Gene Med 2005; **7**: 97–107.
Published online 15 November 2004 in Wiley InterScience (www.interscience.wiley.com). **DOI:** 10.1002/jgm.640

RESEARCH ARTICLE

Antisense downregulation of SARS-CoV gene expression in Vero E6 cells

Yi Shi[1]
Haifeng Luo[1,2]
Jie Jia[1]
Jie Xiong[1]
Dehua Yang[1]
Bing Huang[1]
Youxin Jin[1]*

[1]*State Key Laboratory of Molecular Biology, Institute of Biochemistry and Cell Biology, Shanghai Institutes for Biological Sciences, Chinese Academy of Sciences, People's Republic of China*

[2]*General Surgery Department, Renji Hospital, Shanghai Second Medical University, People's Republic of China*

*Correspondence to: Youxin Jin, State Key Laboratory of Molecular Biology, Institute of Biochemistry and Cell Biology, Shanghai Institutes for Biological Sciences, Chinese Academy of Sciences, Yueyang Road 320, Shanghai 200031, People's Republic of China.
E-mail: yxjin@sibs.ac.cn

Received: 2 February 2004
Revised: 3 May 2004
Accepted: 10 May 2004

Abstract

Background Severe acute respiratory syndrome (SARS) is caused by a novel coronavirus (SARS-CoV). It is an enveloped, single-stranded, plus-sense RNA virus with a genome of ~30 kb. The structural proteins E, M and N of SARS-CoV play important roles during host cell entry and viral morphogenesis and release. Therefore, we have studied whether expression of these structural proteins can be down-regulated using an antisense technique.

Methods Vero E6 cells were transfected with plasmid constructs containing exons of the SARS-CoV structural protein E, M or N genes or their exons in frame with the reporter protein EGFP. The transfected cell cultures were treated with antisense phosphorothioated oligonucleotides (antisense PS-ODN, 20mer) or a control oligonucleotide by addition to the culture medium.

Results Among a total of 26 antisense PS-ODNs targeting E, M and N genes, we obtained six antisense PS-ODNs which could sequence-specifically reduce target genes expression by over 90% at the concentration of 50 μM in the cell culture medium tested by RT-PCR. The antisense effect was further proved by down-regulating the expression of the fusion proteins containing the structural proteins E, M or N in frame with the reporter protein EGFP. In Vero E6 cells, the antisense effect was dependent on the concentrations of the antisense PS-ODNs in a range of 0–10 μM or 0–30 μM.

Conclusions The antisense PS-ODNs are effective in downregulation of SARS. The findings indicate that antisense knockdown of SARS could be a useful strategy for treatment of SARS, and could also be suitable for studies of the pathological function of SARS genes in a cellular model system.

Keywords SARS; antisense technology; Vero E6 cells; RT-PCR; EGFP fusion protein

Introduction

Severe acute respiratory syndrome (SARS) is a newly emerging infectious disease which has caught the attention not only of the scientific community, but also of the public. Infection is usually characterized by fever, dry cough, myalgia, and mild sore throat, which progresses to atypical pneumonia. SARS is caused by a newly identified virus within the family *Coronaviridae* [1–3]. This virus has been designated SARS coronavirus (SARS-CoV) [4]. The overall genome of many SARS-CoV strains has been sequenced. It is an enveloped, single-stranded, plus-sense RNA virus with

a genome of ~30 kb [5,6]. From 1 November 2002 to 31 July 2003, 8098 cases and 774 deaths in 26 countries were reported as a result of SARS by the World Health Organization [7]. Although the initial global outbreak of SARS seems to be under control, SARS will remain a serious concern while there are no suitable measures for curing this disease.

The SARS genome encodes 23 putative proteins and the organization is typical of a coronavirus [5′-replicase (rep), spike (S), envelope (E), membrane (M), and nucleocapsid (N)-3′]. The SARS-CoV rep gene comprises approximately two-thirds of the genome and incorporates a ribosomal slippage site [5,6,8]. Translation without ribosomal frameshifting generates the Orf1a protein and the (−1) frameshift results in translation of the extended Orf1ab polyprotein [8]. These products are then auto-cleaved by the main proteinase ($3CL^{pro}$), which is encoded within the 5′-proximal region of the rep gene [9], to generate several nonstructural proteins including the main proteinase ($3CL^{pro}$), the RNA-dependent RNA polymerase (RdRP) and the RNA helicase. The structural proteins S, E, M and N are common to all known coronaviruses [5]. They function during host cell entry and viron morphogenesis and release [10,11]. During viron assembly, N binds to a defined packaging signal on viral RNA to form the helical nucleocapsid. M is localized at intracellular membrane structures. The interaction between the M and E proteins and nucleocapsids results in budding through the membrane. The S protein is a membranous glycoprotein and is important for viral entry and might define host range, tissue tropism and virulence [12,13].

Antisense technology has become a widely used research tool for the specific inhibition of gene expression. It has attracted considerable attention as a potential therapeutic strategy [14,15]. Antisense oligodeoxynucleotides (ODNs), usually 18–21 nucleotides in length, could sequence-specifically hybridize to the target mRNA through Watson-Crick base pairing to form an mRNA/DNA duplex, which is then degraded by RNAse H, a ubiquitously expressed endonuclease which hydrolyses the RNA strand of the heteroduplex. The antisense ODNs might also physically block mRNA function (e.g. translation) or gene transcription [14]. Therefore, treatment based on an antisense technique only demands knowledge of the DNA sequence of the gene and not of the function of the protein. Antisense ODNs play potential roles in the treatment of many diseases, such as cancer, influenza, AIDS and other diseases [15–21]. The problems of nuclease sensitivity and lower cellular uptake limit antisense oligonucleotides in *in vivo* applications [22]. More stable oligonucleotide derivatives, such as methylphosphonates [23], phosphorothioates [24], and phosphoramidites [25], have been designed. Among these derivatives, phosphorothioate oligonucleotide seems to be a potential antiviral therapeutic agent. In this study, we selected antisense phosphorothioated oligodeoxynucleotide (antisense PS-ODN, 20mer) complementary to 20-base segments within the transcripts of SARS-CoV structural proteins E, M and N.

The purpose of the present study was to establish a model to evaluate the effect of the antisense oligonucleotides on the expression of SARS-CoV gene expression and pick out good target sites within E, M, and N genes for antisense downregulation. We used transiently transfected Vero E6 cells expressing the exon of the E, M, or N protein of SARS-CoV or these exons in fusion with the enhanced green fluorescent protein (EGFP). Cells were then treated with the antisense oligonucleotides used by adding them to the culture medium, which then reached the nuclei and resulted in sequence-specific antisense downregulation of SARS-CoV gene expression.

We conclude that the antisense PS-ODNs could effectively and sequence-specifically downregulate SARS-CoV gene expression in a dose-dependent manner. We obtained six antisense PS-ODNs which could sequence-specifically reduce target gene expression by over 90% at the concentration of 50 μM in the cell culture medium. These findings suggest that antisense technology could be a useful strategy for treatment of SARS, and could also be suitable for studies of the pathological function of SARS genes.

Materials and methods

Construction of plasmids

The E, M and N gene expression vectors (pCDNA3.1/E, pCDNA3.1/M, and pCDNA3.1/N) were constructed and donated by Mr. Youhua Xie (Institute of Biochemistry and Cell Biology, SIBS, CAS). The E, M and N segments were released from these vectors and inserted 5′ to the EGFP gene into the pEGFP-N3 N-terminal 'protein fusion mammalian expression vector' (Clontech) between the EcoR I and BamH I sites. Three plasmid constructs were generated: pEGFP/E, pEGFP/M, and pEGFP/N. All inserts were checked for orientation and correct frame by sequencing.

Cell cultures and transfection

The Vero E6 cells (from the cell bank of the Institute of Biochemistry and Cell Biology, SIBS, CAS) were cultured in Dulbecco's modified Eagle's medium (DMEM), high glucose (Gibco), supplemented with 10% heat-inactivated fetal calf serum (FCS, Hyclone).

The Vero E6 cells were transiently transfected with the plasmid constructs described above with the use of Lipofectamine 2000 (Invitrogen). Following the manufacturer's instructions, the transfection procedures were optimized with respect to relative amounts of DNA and transfection agent and with respect to incubation time. The Vero E6 cells were seeded with 1×10^5 cells in each well of a 24-well plate one day before transfection.

Two μl Lipofectamine 2000 were mixed with 50 μl Opti-MEM I (Invitrogen) and incubated for 5 min at room temperature. 0.8 μg constructs were mixed with 50 μl Opti-MEM I, added to the Lipofectamine 2000/Opti-MEM I mix and incubated for 25 min at room temperature. The cells were washed with DMEM to remove serum and transfected with the construct/Lipofectamine 2000 mix in 500 μl DMEM. After 2 h, the antisense or control oligos were added to the medium. The cell cultures were supplemented with 10% FCS 6 h post-transfection and grew until fluorescence microscopy or harvesting for RT-PCR analysis.

The viability of the cells was tested by removing the cells from the culture plate and counting with a haemocytometer after trypan blue staining. The total number of living and dead cells was then calculated.

Oligodeoxynucleotides

Oligos, phosphorothioate-substituted in all positions, were FPLC-purified (Pharmacia Biotech). The sequences of the antisense oligos are described in Table 1. The scrambled oligo had a randomly chosen sequence.

RNA extraction and RT-PCR analysis

The total RNA of the cells were extracted by using TRIZOL reagent (Invitrogen) and digested by RQ1 DNase (Rnase-free, Promega) at 37 °C for 30 min. The DNase was then heat-inactivated at 65 °C for 10 min. The sequences of the primers for the detection of E gene expression are: 5′ ATGTACTCATTCGTTTCGGAA 3′ (forward) and 5′ TTAGACCAGAAGATCAGGAAC 3′ (reverse). The primers for the M gene are: 5′ ATGTTACTACAATTTGCCTATTC 3′ and 5′ ACGCTCCTAATTTGTAATAAGA 3′. The primers for the N gene are: 5′ ATGTCTGATAATGGACCCCAA 3′ and 5′ GCCAGGAGTTGAATTTCTTGA 3′. The primers for β-actin are: 5′ GTGCCAC CAGACAGCACTGTGTTG 3′ and 5′ TGGAGAAGAGCTATGAGCTGCCTG 3′. Single-tube and one-step RT-PCR were performed with the One-step RNA PCR kit (TaKaRa). Each reaction mixture contained 1× buffer, each deoxynucleotide triphosphate at a concentration of 1 mM, each primer at a concentration of 0.4 μM, $MgCl_2$ at a concentration of 5 mM, 40 U of RNase inhibitor, 5 U of AMV reverse transcriptase, 5 U of AMV-optimized Taq, and 1 μg of extracted RNA brought to a volume of 50 μl with diethyl pyrocarbonate (DEPC)-treated water. After an initial incubation for 30 min at 50 °C followed by denaturation at 94 °C for 4 min, 28 cycles of amplification were performed by using a thermo profile of 94 °C for 30 s and 58 °C for 30 s, with a final extension at 72 °C for 30 s. The amplification products were analyzed by electrophoresis on a 2% agarose gel and stained with ethidium bromide.

Fluorescence microscopy

The Vero E6 cells were seeded on coverslips in the wells of 6-well plates (500 000 cells/well) and transfected as

Table 1. The sequences of the antisense oligos targeting the genes of SARS-CoV structural proteins E, M and N

Target gene	No.	Position in the gene*	Sequence
Small envelope protein (E)	1	26136-26155	5′ AAGTACGCTATTAACTATTA 3′
	2	26168-26187	5′ ACTAGCAAGAATACCACGAA 3′
	3	26212-26231	5′ TCGATTGTGTGCGTACTGCT 3′
	4	26264-26283	5′ CGCGAGTAGACGTAAACCGT 3′
	5	26306-26325	5′ AGAAGATCAGGAACTCCTTC 3′
Membrane protein (M)	6	26415-26434	5′ GCTTAAACAACTCCTGGAAC 3′
	7	26581-26600	5′ TTAATTCTGTAGACAGCAGC 3′
	8	26638-26657	5′ AGCCACATCAAGCCTACAAT 3′
	9	26659-26678	5′ AAGGAAGCAACGAAGTAGCT 3′
	10	26769-26788	5′ CACTTTCCATGAGCGGTCTG 3′
	11	26825-26844	5′ GGAGTGTCCGGCCATTCGCA 3′
	12	26878-26897	5′ GATGTAGCCACAGTGATCTC 3′
	13	26928-26947	5′ CAGTGCCTACACGCTGCGAC 3′
	14	26958-26977	5′ GGTAGCGGTTGTATGCAGCA 3′
	15	26986-27005	5′ AACTATAAATTAAATACAGA 3′
Nucleocapsid protein (N)	16	28112-28131	5′ GTTTGATTGGGGTCCATTAT 3′
	17	28213-28232	5′ GGTCGGCGCTGTTTTGGCCT 3′
	18	28247-28266	5′ GAACCAAGACGCAGTATTAT 3′
	19	28289-28308	5′ AGGGAATCTAAGTTCCTCCT 3′
	20	28372-28391	5′ CGAACTCGTCGGGTAGCTCT 3′
	21	28484-28503	5′ CCATACGATGCCTTCTTTGT 3′
	22	28526-28545	5′ AATGTGGTCTTTGGGTGTAT 3′
	23	28556-28575	5′ ATCCTAATAACAATGCTGCC 3′
	24	28594-28613	5′ TTTGGCAATGTTGTTCCTTG 3′
	25	28864-28883	5′ CGAGGCTTTTTAGATGCCTC 3′
	26	28890-28909	5′ ACTGTTTTGTGGCAGTACGT 3′
Scrambled oligo			5′ TCAACAGGATTGTGGCCTAT 3′

*GenBank accession number NC_004718.

described. After 24 h, cells on the coverslips were fixed in freshly made 4% paraformaldehyde in phosphate-buffered saline (PBS) for 30 min at room temperature. Subsequently, the nuclei were stained with 10 mg/ml DAPI in PBS for 10 min and analyzed using an Olympus BX-50 fluorescence microscope with use of a 10× or 20× objective. The fields were randomly chosen by a sweep across the coverslips under phase contrast illumination. Randomly chosen fields from differently treated cultures in the same experiment were photographed using the same exposure time. The proportion of Vero E6 cells expressing GFP fusion proteins was calculated by counting the number of green fluorescent cells and the total number of cells in the inverted fluorescence microscope.

Results

The uptake of the antisense PS-ODN and its stability in Vero E6 cells

The method of administration of the antisense oligo is crucial for the inhibition effect obtained in Vero E6 cells. The down-regulation effect of antisense PS-ODN added to the culture medium as a free oligonucleotide is varied between different cell types. This could be due to different intracellular concentrations of the PS-ODN, to cell-type-specific differences in the level of RNase H, which is supposed to be a main factor in antisense inhibition of gene expression mediated by PS-ODNs [26]. A FAM-labeled antisense PS-ODN (No.13) was cotransfected with its target gene expression construct (pCDNA3.1/M) to the Vero E6 cells by adding it to the medium directly at a final concentration of 50 μM. The cell cultures were washed with fresh DMEM containing 10% FCS 24 h post-transfection to remove the FAM-labeled PS-ODN. Microscopic examination of the green fluorescence was performed on days 1, 3, and 5 post-transfection (Figure 1). Fluorescence signals were mainly distributed in the cytoplasms after 24 h (Figures 1A and 1B). A nuclear accumulation of PS-ODN was observed in about 5% of the Vero E6 cells. Three and 5 days post-transfection, fluorescence signals could still be observed in the same pattern of distribution (Figures 1C, 1D, 1E, and 1F). These results indicated that the antisense PS-ODN at a high concentration of 50 μM in the culture medium could be taken up by Vero E6 cells and could remain stably in the cytoplasm and the nucleus for a long time.

Screening the antisense oligos that can highly inhibit the expression of the E, M and N genes of SARS-CoV

To study antisense downregulation of the E, M or N gene expression, Vero E6 cells were transiently transfected with constructs containing the exon of the E, M or N gene cloned in the pCDNA3.1 vector. The antisense PS-ODNs were added to the medium after 2 h at a final concentration of 50 μM. The cells were examined 24 h post-transfection for expression of the E, M or N gene by RT-PCR (Figure 2). Six antisense PS-ODNs could reduce target gene expression by over 90% at the concentration of 50 μM (Table 2). They were No.2 and No.4 oligos targeting the E gene of SARS-CoV, No.11 and No.13 oligos targeting the M gene, and No.18 and No.20 oligos targeting the N gene. Only the antisense oligos, but not the scrambled oligo, inhibited expression of SARS-CoV genes. These results indicate a sequence-specific inhibition effect of antisense PS-ODN (20mer).

The antisense oligos inhibited the expression of the E, M and N genes in a dose-dependent manner

Among the 26 antisense PS-ODNs, we selected the six antisense PS-ODNs (No.2, No.4, No.11, No.13, No.18, and No.20) with an inhibition effect over 90% to test if the inhibition effect was dose-dependent. The No.2, No.4, No.13, and No.18 antisense oligos inhibited the expression of the E, M and N genes in a concentration-dependent manner in the range 0–10 μM, while the No.11 and No.20 antisense oligos dose-dependently inhibited target genes expression in the range 0–30 μM (Figure 3). The expression did not vary for increasing concentrations of the scrambled oligo within this range suggesting that the inhibition obtained with the antisense oligo was

Table 2. The inhibition effects of the 26 antisense PS-ODNs targeting the E, M, and N genes of SARS-CoV

Target gene	Antisense PS-ODN	Inhibition activity (%)*
Protein E	No.1	11.5
	No.2	91.8
	No.3	7.5
	No.4	98.1
	No.5	16.6
Protein M	No.6	57.4
	No.7	14.9
	No.8	44.9
	No.9	6.1
	No.10	17.0
	No.11	97.4
	No.12	4.2
	No.13	98.1
	No.14	70.6
	No.15	10.6
Protein N	No.16	16.1
	No.17	12.7
	No.18	94.4
	No.19	10.9
	No.20	97.0
	No.21	21.6
	No.22	79.8
	No.23	57.7
	No.24	72.0
	No.25	16.9
	No.26	52.2

*Data are averaged from three independent experiments.

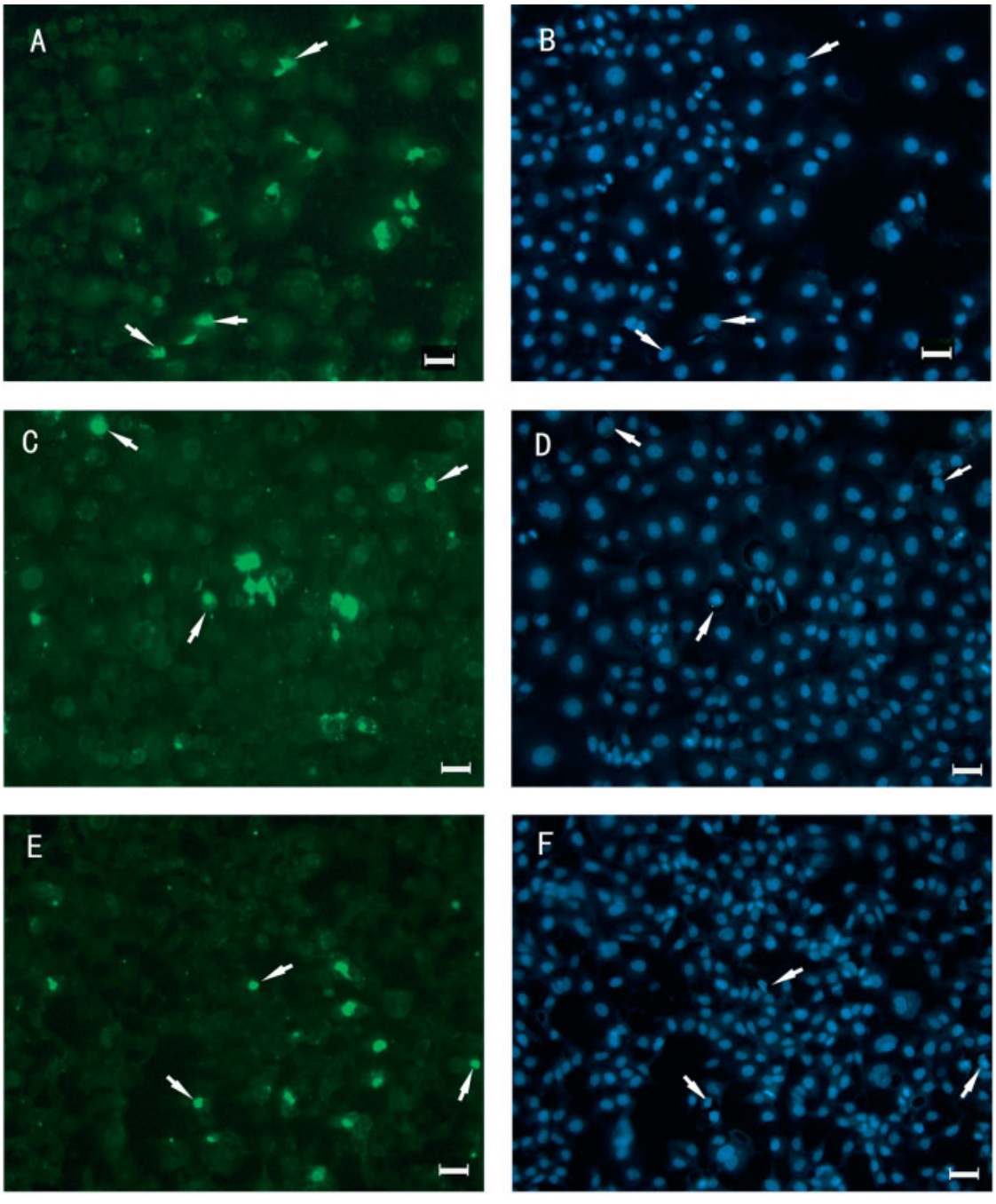

Figure 1. Uptake of the antisense PS-ODN by Vero E6 cells. Vero E6 cells transfected with the construct (pCDNA3.1/M) expressing the M protein of SARS-CoV were treated with FAM-labeled antisense PS-ODN (No.13) at a final concentration of 50 μM in the culture medium. After 24 h, cells were washed with DMEM to remove the FAM-labeled PS-ODN. Fluorescence was examined 1 day (A), 3 days (C), and 5 days (E) post-transfection. The nuclei were stained with DAPI blue in (B), (D), and (F) corresponding to the same microscopic field as (A), (C), and (E), respectively. White arrows indicate the nuclear accumulation of PS-ODN. Scale bar: 40 μm

sequence-specific (Figure 3A). We tested for different toxicities of the oligos in a setup using 2, 10, 30, and 50 μM of the No.13 oligo. The total number of living and dead cells at the termination of the experiment revealed no significant differences between the antisense-treated and the scrambled-treated cultures (Table 3). This indicates that the observed antisense downregulation of SARS-CoV gene expression is not due to toxic effects of these oligos.

Antisense inhibition of expression of the E, M and N proteins fused with EGFP

To further study the antisense inhibition effects, we introduced the antisense PS-ODNs and plasmid constructs containing the exon of the E, M or N gene cloned in frame with the EGFP reporter gene for production of fusion proteins (E-EGFP, M-EGFP and N-EGFP) in Vero

E6 cells (Figure 4). The cells were examined 48 h post-transfection. To show the specificity of the antisense effect, we used scrambled oligo and antisense PS-ODNs targeting other SARS-CoV genes as controls. Microscopic examination of the green fluorescence revealed that the No.2 and No.4 antisense PS-ODNs could reduce the expression of the E-EGFP fusion protein in the cells. However, the No.13 and No.20 antisense PS-ODNs, which could reduce the expression of M-EGFP and N-EGFP, respectively, had no effect on E-EGFP expression (Figures 5A and 5D). The No.11 and No.13 antisense PS-ODNs could reduce the expression of the M-EGFP protein, whereas the No.4 and No.20 antisense PS-ODNs targeting E and N respectively had no effect on M-EGFP (Figures 5B and 5E). The No.18 and No.20 antisense PS-ODNs could reduce the expression of the N-EGFP protein, whereas the No. 4 and No.13 antisense PS-ODNs targeting E and M respectively had no effect on N-EGFP (Figures 5C and 5F). The scrambled oligo had no effect on the expressions of these three EGFP fusion proteins. All these data further proved that the antisense PS-ODNs could specifically block the expression of E, M, and N proteins in mammalian cells.

FAM-labeled antisense PS-ODN had demonstrated that it could remain stably in the cytoplasm and the nucleus for 5 days. Therefore, we tested if the inhibition effect

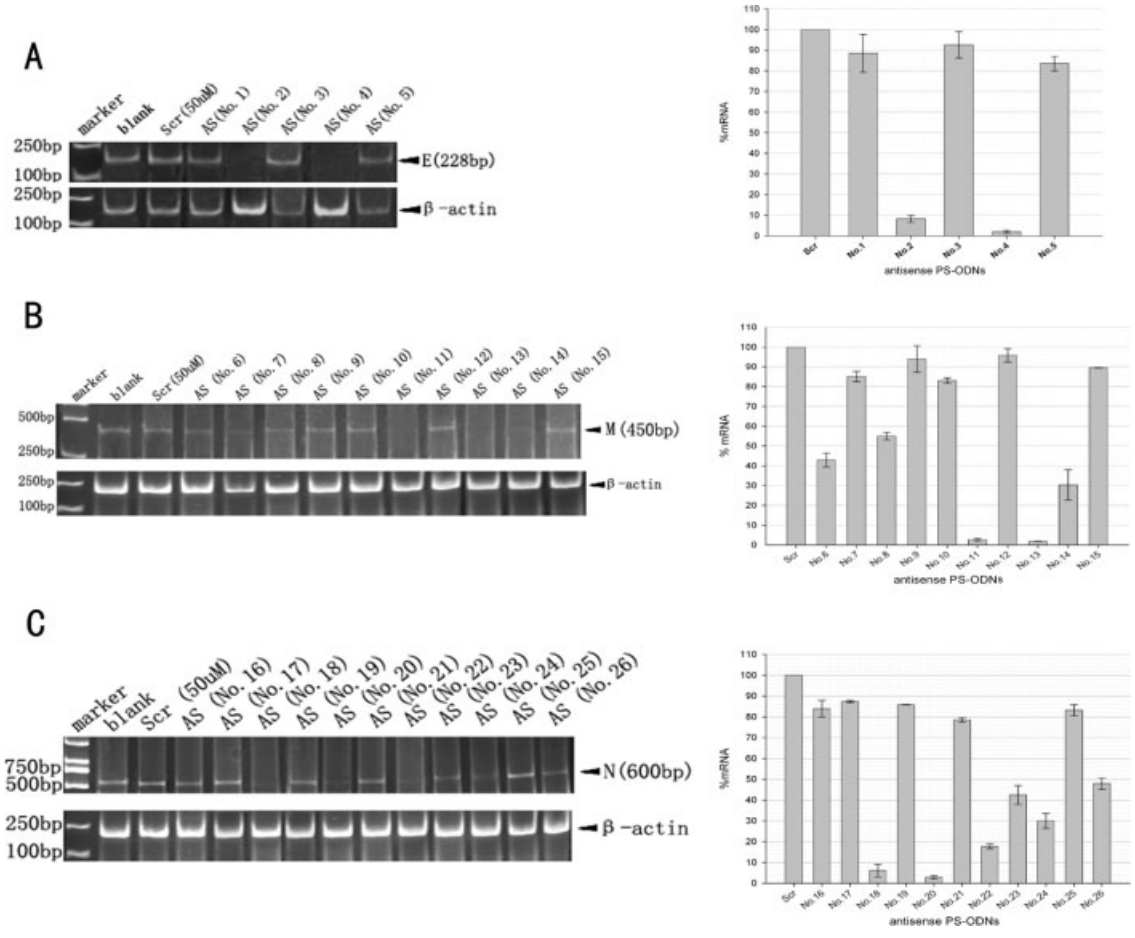

Figure 2. Antisense inhibition of E, M, and N gene expression of SARS-CoV in Vero E6 cells. The cells were cotransfected with the E-, M-, or N-expressing construct and antisense (AS) or scrambled (Scr) oligos at the final concentration of 50 μM in the medium. The cells were harvested 24 h post-transfection and total RNA was extracted for a RT-PCR test. RT-PCR was carried out using E-, M-, and N-specific PCR primer sets (top panel); *β*-actin served as an internal control. After electrophoresis and staining with ethidium bromide, the bands were quantified by densitometry and the E, M, and N levels were corrected for loading differences performed on the *β*-actin results. The scrambled oligo control is set to 100% for each set of transfections. Data are averaged from three experiments with SE indicated. (A) The effects of No.1 to No.5 antisense PS-ODNs on the expression of the SARS-CoV E gene. (B) The effects of No.6 to No.15 antisense PS-ODNs on the expression of the SARS-CoV M gene. (C) The effects of No.16 to No.26 antisense PS-ODNs on the expression of the SARS-CoV N gene

Figure 3. The antisense PS-ODNs inhibit SARS-CoV gene expression in a concentration-dependent manner. The cells were cotransfected with the SARS-CoV genes expressing constructs and antisense (AS) or scrambled (Scr) oligos in different concentrations. The cells were harvested 24 h post-transfection and total RNA was extracted for RT-PCR examination. (A) The inhibition of E gene expression by No.2, No.4 antisense oligos or scrambled oligo at different concentrations. (B) The inhibition of M gene expression by No.11 or No.13 antisense oligo at different concentrations. (C) The inhibition of N gene expression by No.18 or No.20 antisense oligo at different concentrations. The dose-dependent inhibition graphs are shown under the gel image. Each point is the mean ±SD of four independent experiments

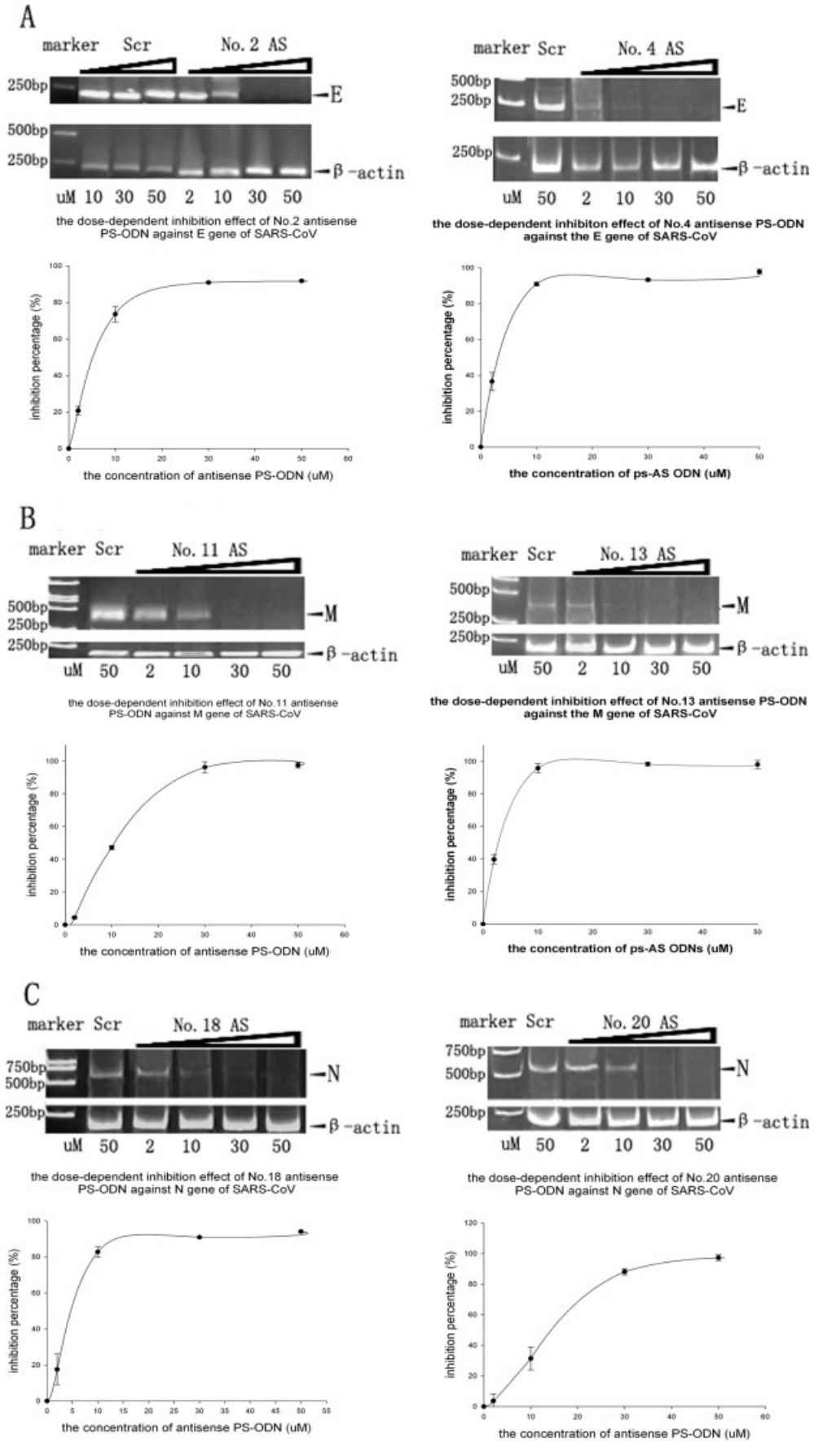

Table 3. Cellular toxicity of the antisense and scrambled oligos

Type and concentration of oligo	Total number of cells per culture after 24 h**
None*	4.68×10^5
2 μM antisense (No.13)	4.50×10^5
10 μM antisense (No.13)	3.63×10^5
30 μM antisense (No.13)	4.21×10^5
50 μM antisense (No.13)	3.86×10^5
2 μM scrambled	4.38×10^5
10 μM scrambled	4.10×10^5
30 μM scrambled	3.65×10^5
50 μM scrambled	4.02×10^5

*Transfection was carried out with pCDNA3.1/M alone.
**Number of cells seeded in each well of a 6-well cell culture plate was 5.0×10^5. Viability staining showed $\leq$10% dead cells in all cultures at the end of the experiment (24 h).

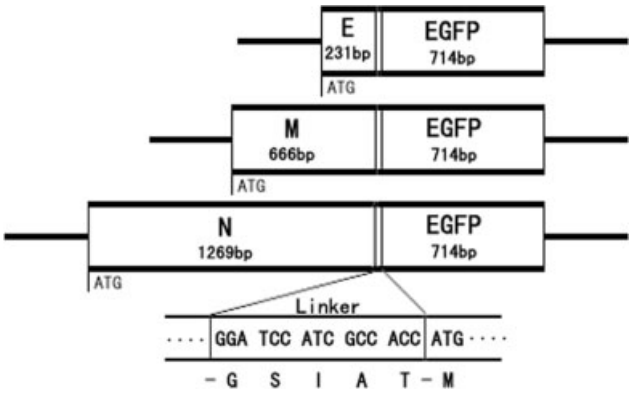

Figure 4. Scheme of the EGFP-E, EGFP-M, and EGFP-N DNA constructs. The ORFs of E, M, and N were linked to the coding sequence of enhanced green fluorescent protein (EGFP). A flexible linker encoding five amino acids was introduced between the EGFP and E, M, or N genes

could last for such a long time. Vero E6 cells transfected with pEGFP/E were treated with No.4 antisense oligo or scrambled oligo added to the culture medium at the final concentration of 10 μM for 24 h and the cells were washed with DMEM to remove the oligo. After washing the cells were grown in DMEM supplemented with 10% FCS. Both microscopic examination and the RT-PCR test indicated the inhibition effect could last for 5 days too (Figure 6).

Discussion

The genome of coronavirus encodes 23 putative proteins, including four major structural proteins; nucleocapsid (N), spike (S), membrane (M), and small envelope (E), which play essential roles during host cell entry, viral morphogenesis and release [10,11]. These structural proteins were attractive targets for the development of an anti-SARS agent. Among these proteins, we selected E, M, and N as the targets of antisense oligos. A characteristic of RNA viruses is the high rate of genetic mutation, which leads to evolution of new viral strains and is a mechanism by which viruses escape host defenses. The spike protein, a glycoprotein projection on the viral surface, was crucial for viral attachment and entry into the host cell. In addition, variations of S protein among strains of coronavirus are responsible for host range and tissue tropism [27]. China confirmed a new case of SARS on January 5, 2004. It is the country's first new case since the outbreak last year. The results of genetic sequencing of samples from the latest patient with SARS show that variation of the S gene existed in this SARS-CoV strain [28]. Since the S1 subunit of the spike protein is the major antigenic moiety for coronaviruses and is not an essential structural protein, it is prone to high mutation rates as the virus evolves in host populations [29]. Therefore, we have not chosen the S protein as a target of antisense oligos. In this work, we have evaluated the down-regulation effects of 26 antisense PS-ODNs targeting different sites along the open reading frames (ORFs) of E, M, and N proteins and obtained 12 antisense oligos which could reduce target gene expression by over 50% in Vero E6 cells at the concentration of 50 μM in the culture medium. Therefore, we could have many choices when one target site is mutated.

Human coronaviruses are usually difficult to culture *in vitro*, whereas most animal coronaviruses and SARS-CoV can be easily cultured in African green monkey kidney (Vero E6) cells [30]. Direct cytopathic effects of SARS-CoV could be demonstrated on inoculating the viral isolates into Vero E6 cells [3,5,31], which makes Vero E6 cells a suitable model for the study of the antisense effect. Because SARS is dangerous for its high morbidity and mortality rates, it is safer and more convenient to study anti-SARS agents by using Vero E6 cells transfected with SARS-CoV gene expression vectors. In this cell model, we obtained an antisense sequence-specific downregulation of SARS-CoV gene expression as seen from the results of RT-PCR and from a reduced fluorescence intensity of EGFP to which the SARS-CoV protein E, M, or N was fused.

A problem in the use of antisense oligonucleotides is their inefficient cellular uptake. They are found mainly in endosomes and lysosomes [32,33]. Therefore, we used high concentrations of the free antisense PS-ODNs in the cell culture medium to increase the intracellular concentrations of the PS-ODNs. In experiments with FAM-labeled antisense oligos in concentrations of 50 μM, we observed that most Vero E6 cells internalized antisense oligos in the cytoplasm and about 5% of the Vero E6 cells showed nuclear uptake of the oligo. The FAM-labeled PS-ODN also showed high stability in Vero E6 cells. In accordance with this, we obtained a long antisense downregulation effect in Vero E6 cells. As antisense PS-ODNs may not work well in *in vivo* treatment of diseases because of a fast breakdown and of possible toxicity, more suitable antisense oligonucleotide derivatives have been developed for therapeutic use, for example, NeuGenes antisense compounds

(AVI Biopharma [34]) and locked oligonucleotides. They displayed advantageous pharmaceutical properties in stability, specificity, efficacy, delivery and safety. However, the PS-ODNs can play an important role in further studies of pathological functions of SARS genes in the Vero E6 cell model for a future treatment and cure.

Taken together, we have found some good target sites for antisense downregulation of SARS-CoV gene expression. Our present results indicate a sequence-specific down-regulation effect of antisense PS-ODN (20mer) in Vero E6 cells, and we found an effective range of concentrations, where the antisense oligo inhibited expression of the E, M, and N genes of SARS-CoV in a concentration-dependent manner. The antisense PS-ODNs can be developed into effective anti-SARS agents. Besides being a potential therapeutic

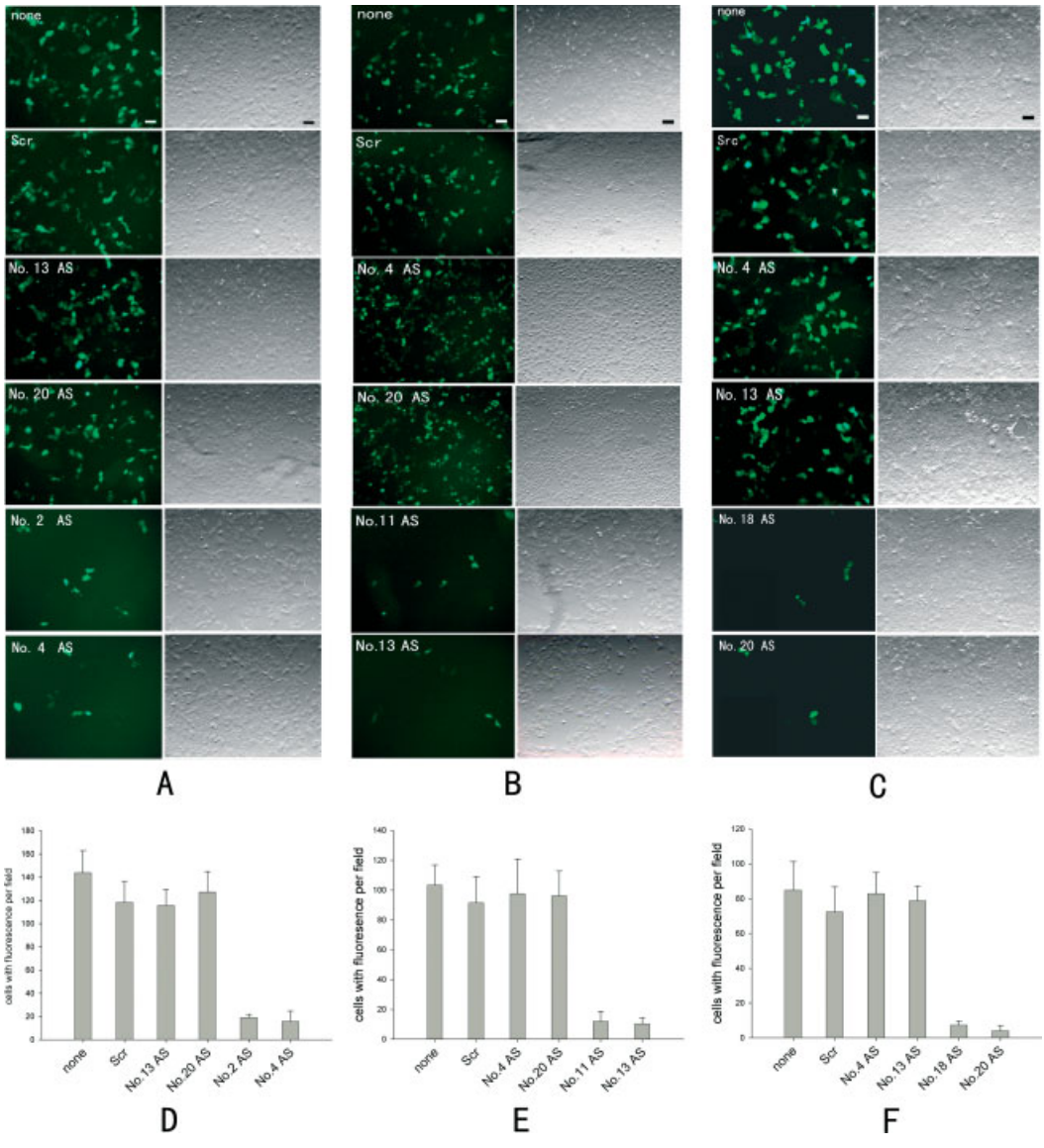

Figure 5. Effect of antisense PS-ODNs on expression of E-EGFP, M-EGFP, and N-EGFP fusion proteins in Vero E6 cells. Fluorescence micrographs of cells transfected with GFP fusion protein expression constructs and treated with scrambled oligo (Scr), antisense oligos (AS), or no oligo (none) added to the culture medium for 48 h. Phase contrast micrographs of the same fields are shown in the right-hand row. (A) Downregulation of expression of E-EGFP fusion protein by No.2 and No.4 antisense oligos. (B) Downregulation of expression of M-EGFP fusion protein by No.11 and No.13 antisense oligos. (C) Downregulation of expression of E-EGFP fusion protein by No.18 and No.20 antisense oligos. (D, E, F) Number of cells per field of view expressing detectable EGFP fusion protein. An average from four fields is shown for each transfection. Data are from a representative experiment. Scale bar: 100 μm

Figure 6. Effect of No.4 antisense PS-ODN on expression of E-EGFP fusion protein in Vero E6 cells from days 1 to 5. Vero E6 cells transfected with pEGFP/E were treated with No.4 antisense oligo (No.4 AS) or scrambled oligo (Scr) added to the culture medium at a final concentration of 10 μM for 24 h and the oligos were removed by washing the cells with fresh DMEM containing 10% FCS. Fluorescence micrographs at 1 day, 3 days, and 5 days are shown in (A). Phase contrast micrographs of the same fields are shown in the right-hand row. Scale bar: 100 μm. Numbers of cells per field of view expressing detectable EGFP fusion protein are shown in (B). An average from four fields is shown for each transfection. The total RNA was extracted for RT-PCR examination (C, D)

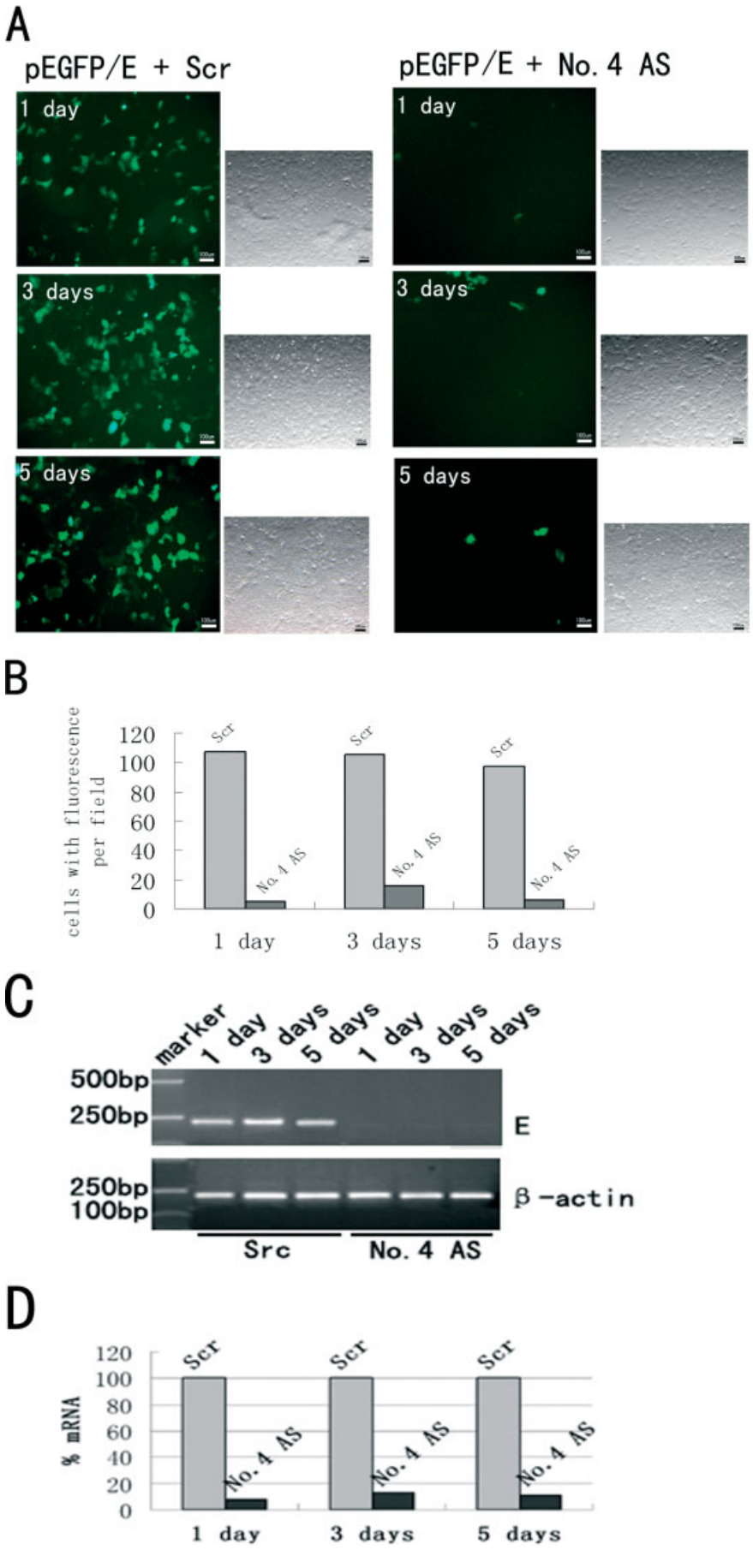

tool, antisense oligonucleotides provide a highly selective means to study the pathological functions of SARS-CoV genes.

Acknowledgements

We thank Professor Xirui Ge for giving us the Vero E6 cell line and Dr. Youhua Xie for donating us three plasmids: pCDNA3/E, pCDNA3/M, and pCDNA3/N. This work was supported by Grant No. 2003AA208215 from the National High Technology Programs of China and Grant No. 03DZ14103 from the Science and Technology Commission of Shanghai Municipality.

References

1. Drosten C, Gunther S, Preiser W, *et al*. Identification of a novel coronavirus in patients with severe acute respiratory syndrome. *New Engl J Med* 2003; **348**: 1967–1976.
2. Ksiazek TG, Erdman D, Goldsmith CS, *et al*. A novel coronavirus associated with severe acute respiratory syndrome. *New Engl J Med* 2003; **348**: 1953–1966.
3. Peiris JSM, Lai ST, Poon LL, *et al*. Coronavirus as a possible cause of severe acute respiratory syndrome. *Lancet* 2003; **361**: 1319–1325.
4. World Health Organization. Update 31: coronavirus never before seen in humans is the cause of SARS. April 16, 2003; Available: http://www.who.int/csr/sarsarchive/2003_04_16/en/ (accessed May 2, 2003).
5. Rota PA, Oberste MS, Monroe SS, *et al*. Characterization of a novel coronavirus associated with severe acute respiratory syndrome. *Science* 2003; **300**: 1394–1399.
6. Marra MA, Jones SJM, Astell CR, *et al*. The genome sequence of the SARS-associated coronavirus. *Science* 2003; **300**: 1399–1404.
7. Available: http://www.who.int/csr/sars/country/en.
8. Lai MM, Cavanagh D. *Adv Virus Res* 1997; **48**: 1–100.
9. Ziebuhr J, Snijder EJ, Gorbalenya AE. *J Gen Virol* 2000; **81**: 853–879.
10. *The Coronaviridae*, Siddell SG (ed). Plenum: New York, 1995.
11. *Fields Virology* (4th edn). Fields BN, Knipe DM, Howley PM, Griffin DE (eds). Lippincott Williams & Wilkins: Philadelphia, 2001.
12. Philips JJ, Chua MM, Rall GF, *et al*. Murine coronavirus spike glycoprotein medicates degree of viral spread, inflammation and virus-induced immunopathology in the central nervous system. *Virology* 2002; **301**: 109–120.
13. Gallagher TM, Buchmeier MJ. Coronavirus spike proteins in viral entry and pathogenesis. *Virology* 2001; **279**: 371–374.
14. Gibson I. Antisense DNA and RNA strategies: new approaches to therapy. *J R Coll Physicians Lond* 1994; **28**: 507–511.
15. Dean NM, Bennett CF. Antisense oligonucleotide-based therapeutics for cancer. *Oncogene* 2003; **22**: 9087–9096.
16. Mizuta T, Fujiwara M, Hatta T, *et al*. Supression of influenza A virus growth in mice by a PB2-as antisense oligonucleotide. *Nat Biotechnol* 1999; **17**: 583–587.
17. Zerial A, Thuong NT, Helene C. Selective inhibition of the cytopathic effect of type A influenza virus by oligonucleotides covalently linked to an intercalating agent. *Nucleic Acids Res* 1987; **5**: 9909–9919.
18. Matsukura M, Zon G, Shinozuka M, *et al*. Regulation of viral expression of HIV in vitro by an antisense phosphorothioate oligodeoxynucleotide against rev in chronically infected cells. *Proc Natl Acad Sci U S A* 1989; **86**: 4244–4248.
19. Kim S-G, Suzuki Y, Nakashima H, *et al*. Phosphorothioate analogues of oligodeoxyribonucleotides: synthesis and activity as inhibitors of replication of human immunodeficiency virus. *Biochem Biophys Res Commun* 1991; **179**: 1614–1619.
20. Kim S-G, Kanbara K, Nakashima H, *et al*. Anti-HIV activities and physicochemical properties of phosphorothioate analogues complementary to HIV sequences. *Bioorg Med Chem Lett* 1993; **3**: 1223–1228.
21. Zamecnik PC, Stephenson ML. Inhibition of Rous sarcoma virus replication and transformation by a specific oligodeoxynucleotide. *Proc Natl Acad Sci U S A* 1978; **75**: 280–286.
22. Hélène C, Toulmé JJ. Specific regulation of gene expression by antisense, sense and antigene nucleic acids. *Biochem Biophys Acta* 1990; **149**: 99–125.
23. Miller PS, Agris CH, Aurelian L, *et al*. Control ribonuleic acid function by oligonucleotide methylphosphonates. *Biochimie* 1985; **67**: 769–776.
24. Stec W, Zon G, Egan W, *et al*. Automated solid-phase synthesis, separation, and stereochemistry of phosphorothioate analogs of oligodeoxyribonucleotides. *J Am Chem Soc* 1984; **106**: 6077–6079.
25. Agrawal S, Goodchild J, Civeira MP, *et al*. Phosphoramidate, phosphorothioate, and methylphosphonate analogs of oligodeoxynucleotide: inhibitors of replication of human immunodeficiency virus. *Nucleosides Nucleotides* 1989; **8**: 819–823.
26. Anneloor LM, ten Asbroek A, van Groenigen M, *et al*. The involvement of human ribonucleases H1 and H2 in the variation of response of cells to antisense phosphorothioate oligonucleotides. *Eur J Biochem* 2002; **269**: 583.
27. Kuo L, Godeke GJ, Raamsman MJ, Masters PS, Rottier PJ. Retargeting of coronavirus by substitution of the spike glycoprotein ectodomain: crossing the host cell species barrier. *J Virol* 2000; **74**: 1393–1406.
28. Jane Parry. WHO confirms SARS in Chinese journalist. *Br Med J* 2004; **328**: 65, doi:10.1136/bmj.328.7431.65.
29. Ruan Y-J, Wei CL, Ee LA, *et al*. Comparative full-length genome sequence analysis of 14 SARS coronavirus isolates and common mutations associated with putative origins of infection. *Lancet* 2003; **361**: 1779–1785.
30. Drosten C, Günther S, Preiser W, *et al*. Identification of a novel coronavirus in patients with severe acute respiratory syndrome. *N Engl J Med* 2003; **348**: 1967–1976.
31. Ng ML, Tan SH, See EE, *et al*. Proliferative grown of SARS coronavirus in Vero E6 cells. *J Gen Virol* 2003; **84**: 3291–3303.
32. Stein CA, Cheng YC. Antisense oligonucleotides as therapeutic agents – is the bullet really magical? *Science* 1993; **261**: 1004–1012.
33. Stein CA, Krieg AM. Problems in interpretation of data derived from in vitro and in vivo use of antisense oligodeoxynucleotides. *Antisense Res Dev* 1994; **4**: 67–69.
34. Available: http://www.avibio.com/neugene.html.

